Journal of Solid State Chemistry **146,** 114–123 (1999)
Article ID jssc.1999.8316, available online at http://www.idealibrary.com on IDEAL®

Neutron and X-Ray Structure Refinements between 15 and 1073 K of Piezoelectric Gallium Arsenate, $GaAsO_4$: Temperature and Pressure Behavior Compared with Other α-Quartz Materials

E. Philippot,*,[1] P. Armand,* P. Yot,* O. Cambon,* A. Goiffon,* G. J. McIntyre,† and P. Bordet‡

*Laboratoire de Physicochimie de la Matière Condensée, CNRS- UMR 5617, Université de Montpellier II, cc 003, Place E. Bataillon, F-34095 Montpellier Cedex 5, France; †Institut Laue-Langevin, B.P. 156, F-38042 Grenoble Cedex 9, France; and ‡Laboratoire de Cristallographie, CNRS, BP 166, F-38042 Grenoble Cedex 9, France

Received January 20, 1999; in revised form March 25, 1999; accepted April 18, 1999

Previous X-ray crystal structure refinement of $GaAsO_4$ gave spurious As–O (1.72 Å) and Ga-O (1.77 Å) bond distances by comparison with theoretical values and with experimental values from $AlAsO_4$ and $GaPO_4$ ([As–O] ≅ 1.67 Å and [Ga–O] ≅ 1.82 Å). Therefore, a complete structural reinvestigation of gallium arsenate was carried out between 15 and 1073 K by both neutron and X-ray diffraction. All new analyses led to experimental bond values in agreement with those predicted, i.e., close to 1.67 and 1.82 Å. This new structural investigation of $GaAsO_4$ over a wide range of temperatures emphasizes the high thermal stability of the α-quartz packing in this compound, the best amongst quartz-like materials. The experimental relation between structural deformation and piezoelectric properties of these quartz-like materials also allows us to predict that $GaAsO_4$ would have the best piezoelectric characteristics for its AT-cut. Conversely, its higher covalent character should imply a greater pressure sensitivity, with a crystal structure transition around 9 GPa. Thus, $GaAsO_4$ would be the best piezoelectric candidate for high temperature applications but not for high pressure devices. © 1999 Academic Press

INTRODUCTION

For many years, we have been studying piezoelectric quartz-like materials (notably the crystal growth, physical characterization, and crystal structure) (1–3). In addition to α-quartz itself, this family is composed of GeO_2 and compounds with the general formula $M^{III}X^{V}O_4$ where M = Al, Ga, Fe, B, … , and X = P and As. The α-quartz structure, space group $P3_121$ (or $P3_221$), is built up of left-handed (or right-handed) helical chains of AO_4 tetrahedra ($A = M$ or X) parallel to the c-axis, interconnected to describe a three-dimensional network. Each MO_4 tetrahedron shares its four corners with XO_4 tetrahedra (and vice versa). The c parameter for $M^{III}X^{V}O_4$ crystals is twice the c parameter of SiO_2 and GeO_2 because Si or Ge atoms are alternately replaced by M and X atoms, displaced approximately by $c/2$ (Fig. 1). The equivalent positions of all heavy atoms (M and X) are 3a (x, 0, 1/3) and 3b in $P3_121$ (x, 0, 5/6), respectively, with approximately the same x value ($x \approx 0.45$).

Ten years ago, most of the crystal structures of this family were investigated by X-ray diffraction (1). More recently, we tried to relate the structural distortions of these phases, in terms of the M–O–X angle values (θ), to their physical behavior (existence of the $\alpha \leftrightarrow \beta$ transition (2), piezoelectric properties (3)). For very well-characterized crystals (SiO_2, $AlPO_4$, and $GaPO_4$), it proved possible to relate linearly their M–O–X values (143.7, 142.8, and 134.6° respectively) to the existence and temperatures of the $\alpha \leftrightarrow \beta$ transition and to their piezoelectric properties and, by extrapolation, to anticipate the unknown characteristics of materials for which the growth of large crystals is not yet controlled. Thus, $GaAsO_4$ and GeO_2, which have the most distorted structures ([M–O–X] = 129.9° and 130.1°, respectively, compared to the ideal angle close to 154° in β-quartz (4)), seem to be the most promising materials with regard to piezoelectric properties.

However, for $GaAsO_4$, some details of the crystal structure, determined by X rays, appear spurious (1). For example, the As–O bond distances ([As–O] = 1.72 Å) seem to be too long and, conversely, the Ga–O distances ([Ga–O] = 1.77 Å) appear to be too short if we compared them to Shannon and Prewitt's theoretical values (5) (1.68 and 1.82 Å for As–O and Ga–O respectively) and to the distances encountered in $GaPO_4$ ([Ga–O] = 1.81 Å) and in $AlAsO_4$ ([As–O] = 1.66Å) (1).

What might be the explanation? First, the heavy gallium and arsenic atoms have the same electronic environment ($Ga^{3+} = As^{5+} = 28$ electrons giving very similar X-ray scattering factors) and, thus, they cannot be easily differentiated by X-ray diffraction (ordering of As and Ga in the

[1] To whom correspondence should be addressed.

0022-4596/99 $30.00
Copyright © 1999 by Academic Press
All rights of reproduction in any form reserved.

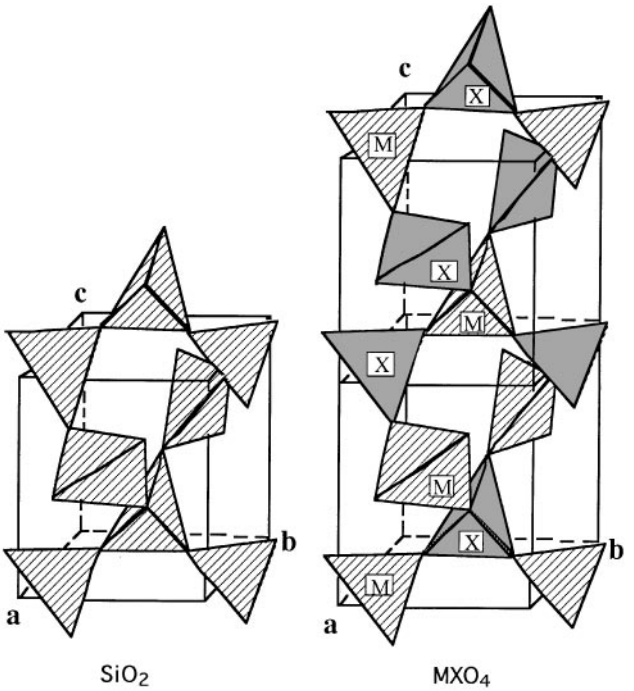

FIG. 1. Comparison of the crystal structures of α-quartz and α-MXO_4 quartz-like materials.

MXO_4 structure should give rise to reflections of the type $l = 2n + 1$, yet only one of these gave an observable reflection in the X-ray experiment).

Secondly, the increase of the structural distortion might induce the formation of twins (optical and electrical twins or Dauphiné and Brazil twins) which are difficult to detect, even in polarized light. The most frequent twin corresponds to the coexistence of small left- and right-handed domains (or $P3_121$ and $P3_221$ domains).

Either of these factors may explain why the two heavy atoms had not been well distinguished in the previous structural investigation and could lead to apparently incorrect Ga–O and As–O bond lengths (1). To solve this problem, we performed a neutron diffraction investigation, at room temperature. Indeed, if the differentiation of Ga and As atoms is difficult by X-ray diffraction, it should be possible by neutron diffraction where the scattering lengths for Ga and As are 7.288 and 6.58×10^{-13} cm, respectively. Thus, it should be possible to decide between these hypotheses, and, consequently, determine the correct lengths of the Ga–O and As–O bonds in $GaAsO_4$.

Moreover, since the piezoelectric properties of the AT-compensated cut (cut with zero frequency shift in terms of temperature) seem to be linearly related to the crystal structure distortion in terms of the M–O–X angle (θ) (3), the stability of these properties is directly related to the stability of the structure. In other words, the more constant is the θ value with the temperature, the more stable are the piezoelectric properties. As both this neutron investigation and the previous X-ray study lead to the same θ value at room temperature ([129.6°] and [129.9°](1), respectively), regardless of the apparent inconsistencies in the Ga–O and As–O bond lengths, further X-ray diffraction measurements have been made between 15 and 1073 K to check the sensitivity of the bridging angle.

EXPERIMENTAL

Neutron Diffraction Data Collection

The crystal used for the neutron data collection, obtained from the horizontal temperature gradient method described elsewhere (6), was an oblique prism with faces (1 0 −1 1), (−1 0 1 −1), (−1 1 0 1), (0 −1 1 1), and (1 0 −1 −2) and all edges about 4 mm long. The data were collected on the four-circle diffractometer D9 at the Institut Laue-Langevin (Grenoble, France) in a beam of wavelength 0.8411(1) Å obtained by reflection from a Cu (220) monochromator and calibrated against reflections from a Ge single crystal. This diffractometer is equipped with a small two-dimensional area detector (7) which allows optimal delineation of the weaker peaks from the general background. One or two equivalents were scanned for most unique reflections to $\sin\theta/\lambda = 0.97$ Å^{-1} at both 295 and 15 K. For the data collection at 15 K, the temperature was maintained by a Displex cryo-refrigerator. The reflections with $l = 2n + 1$, which were not observed in the previous X-ray experiment, were clearly visible at both temperatures, although they were generally considerably weaker than the $l = 2n$ reflections.

Background corrections following Wilkinson *et al.* (8) and Lorentz corrections were applied. Absorption correction and calculation of the mean path length for each reflection were by Gaussian integration (9) using the calculated absorption coefficient $\mu = 0.00431$ mm^{-1}; the transmission range was 0.9863–0.9923. Averaging in space group $P3_121$ gave 904/1157 unique reflections, with agreement index $R_w = 0.017/0.021$ at 295/15 K. Because the three-dimensional count distribution around every reflection was observed, the centroids of all scanned reflections could be found. Least-squares matching of the observed and calculated centroids of the 1080/1290 strongest reflections at 295/15 K gave the cell parameters $a = 4.9942(3)/4.9940(1)$ Å and $c = 11.3816(13)/11.3871(4)$ Å. These values do not include the estimated uncertainty in the wavelength.

The structure was refined using the full-matrix least-squares program UPALS described by Lundgren (10). The quantity minimized was $\sum w(|F_o|^2 - |F_c|^2)^2$, where $w^{-1} = \sigma^2_{count}(|F_o|^2) + k^2|F_o|^2$, and σ^2_{count} was derived by Poisson counting statistics. The constant k was fixed at 0.01. The scattering lengths for Ga, As, and O were 7.288, 6.58, and 5.803×10^{-13} cm, taken from Sears (11). Extinction affected a considerable fraction of the reflections in this rather perfect and large crystal, but could be well-accounted for

by a Becker and Coppens (12, 13) type-I model with a Lorentzian distribution of mosaic blocks. Because of the differing mean path lengths amongst repeated measurements of the same reflection and amongst equivalent reflections, and the consequent differing degrees of reduction by extinction, the refinement of the structure was made against the unmerged data. Thirty parameters were adjusted in the final refinements at both temperatures: scale factor, mosaic width, and positional and anisotropic displacement parameters for all four unique atoms. The cell parameters are summarized in Table 1 and the confidence factors obtained after convergence in Table 2.

X-ray Data Collection

For the X-ray data collection, crystals of $GaAsO_4$ were grown hydrothermally from a saturated solution of $Ga(OH)_3$ in arsenic acid at room temperature (1). One single crystal was selected and ground to a sphere of 0.1 mm radius. Nine data collections were carried out between room temperature and 1073 K, at 100 K intervals, on a KappaCCD Nonius diffractometer using graphite-monochromatized Ag$K\alpha$ radiation. The high temperatures were achieved by using a homemade air blower, with the air stream directed horizontally and perpendicular to the X-ray beam. The crystal to detector distance was 35 mm. The CCD data collections were made by the rotation technique: 90 successive images of 2 degrees each were recorded at a speed of 1/15deg/s about the vertical ϕ axis, with the CCD detector perpendicular to the beam direction. Each image was collected twice in order to detect and eliminate electronic parasites ("zingers"). The CCD images were treated by using the Denzo-SMN software (14). The Bragg reflection intensities were indexed, integrated, and averaged in the $P3_121$ space group. The Rsym values, which describe the mean statistical intensity distribution of equivalent reflections in the space group averaging process, were in the 4–5% range for all data collections, with ≈190 independent reflections, of which ≈180 satisfied $I > 0$. The combination of X-ray wavelength, detector dimensions, and crystal-to-detector distance led to a maximum value for $\sin\theta/\lambda$ of 0.64. A spherical absorption correction ($\mu R = 0.96$) was applied.

TABLE 1
Unit-Cell Parameters of $GaAsO_4$ from Neutron (*) and X-Ray Diffraction Data at Different Temperatures

	a (Å)	c (Å)	V (Å^3)
15*	4.9940(1)	11.3871(4)	245.9(1)
295*	4.9942(4)	11.3816(13)	245.8(1)
293	*4.993(1)*	*11.366(2)*	*245.4(2)*
289	4.997(1)	11.379(3)	246.1(2)
373	5.007(1)	11.391(3)	247.3(2)
473	5.011(1)	11.388(3)	247.6(2)
573	5.017(1)	11.401(3)	248.5(2)
673	5.025(1)	11.408(3)	249.5(2)
773	5.033(1)	11.411(3)	250.3(2)
873	5.040(1)	11.408(3)	251.0(2)
973	5.051(1)	11.421(3)	252.3(2)
1073	5.059(1)	11.424(3)	253.2(2)

Note. Previous refinement from X-ray data (1) are in italics.

TABLE 2
The Confidence Factors Obtained after Convergence for Neutron (*) and X-Ray Refinements at Different Temperatures

T (K)	wR(F^2)	Goodness of fit	R(F)	Total reflections	Reflections used	Unique reflections
15*	0.073	4.61	0.025	1609	1596	1157
295*	0.048	2.57	0.019	1560	1545	896
289	0.046	3.48	0.028		270	
373	0.046	3.88	0.033		174	
473	0.049	5.81	0.042		177	
573	0.046	5.10	0.045		178	
673	0.046	4.99	0.036		179	
773	0.046	5.10	0.034		178	
873	0.048	5.37	0.043		176	
973	0.050	5.45	0.039		183	
1073	0.052	6.01	0.044		182	

The refinements were carried out by using the MXD software (15), starting from the parameters obtained in Ref. (1). All reflections with $I > 0$ were used, and the weighting scheme was taken from counting statistics ($w = 1/\sigma^2$). For example, for the 373 K data collection, 174 reflections were used, comprising 89 superstructure reflections with l odd, among which 14 had $I > 10\sigma$. Secondary extinction effects were taken into account by using the model from Becker and Coppens (12) for isotropic extinction of type I, with a Lorentzian distribution. The positional and anisotropic thermal parameters of all atoms were refined, leading to 30 variables including the scale factor and extinction parameter. The number of superstructure reflections observed proved to be sufficient to lead to a correct description of the cation ordering along the c axis. It is worth noting that the superstructure reflection intensities are essentially due to the ordered oxygen anion displacements around the Ga and As cations, rather than to the difference in scattering power between these two types of cations, which is very small and probably not directly observable with X-ray diffraction techniques. The confidence factors obtained after convergence were w$R(F^2) \approx 5\%$ and $R(F) \approx 4\%$ for all temperatures. The cell, positional, and thermal parameters are given in Tables 1, 3, and 4, respectively. Table 4 also includes the thermal parameters from the two neutron refinements.

RESULTS

Neutron Diffraction Refinements

Table 5 summarizes the characteristic angles and bond distances of $GaAsO_4$ at 15 and 295 K compared to those

TABLE 3
Final Atomic Coordinates of $GaAsO_4$ from neutron (*) and X-ray Data Refinements at Different Temperatures

T (K)	x (Ga)	x (As)	x (O_1)	y (O_1)	z (O_1)	x (O_5)	y (O_2)	z (O_2)
15*	0.44991(7)	0.44800(8)	0.39848(9)	0.31858(9)	0.38307(3)	0.39674(9)	0.29595(9)	0.87152(3)
295*	0.45092(5)	0.44933(6)	0.39910(6)	0.31683(6)	0.38363(2)	0.39816(6)	0.29426(6)	0.87213(2)
293	*0.4504(2)*	*0.4499(2)*	*0.400 (2)*	*0.309(1)*	*0.3808(4)*	*0.399(2)*	*0.304(1)*	*0.8755(4)*
289	0.4516(2)	0.4494(2)	0.3997(9)	0.3181(8)	0.3838(2)	0.398(1)	0.2929(9)	0.8716(3)
373	0.4523(3)	0.4496(3)	0.400(1)	0.315(1)	0.3838(3)	0.400(1)	0.293(1)	0.8720(4)
473	0.4521(3)	0.4505(3)	0.400(1)	0.317(1)	0.3842(3)	0.400(1)	0.291(1)	0.8725(4)
573	0.4526(3)	0.4516(3)	0.401(1)	0.315(1)	0.3844(3)	0.400(1)	0.291(1)	0.8724(4)
673	0.4533(3)	0.4522(3)	0.401(1)	0.315(1)	0.3846(3)	0.402(1)	0.290(1)	0.8730(4)
773	0.4537(3)	0.4531(3)	0.401(1)	0.314(1)	0.3849(3)	0.402(1)	0.291(1)	0.8732(4)
873	0.4542(3)	0.4539(3)	0.401(2)	0.312(1)	0.3851(3)	0.402(1)	0.289(1)	0.8736(4)
973	0.4548(3)	0.4549(3)	0.400(2)	0.309(2)	0.3853(4)	0.404(2)	0.289(2)	0.8736(5)
1073	0.4557(4)	0.4554(4)	0.403(2)	0.311(2)	0.3856(4)	0.404(2)	0.286(2)	0.8745(5)

Note. Previous refinement from X-ray data (1) are in italics.

previously obtained from X-ray refinement (1). The first important difference lies in the length variation of the Ga–O and As–O bonds with a lengthening of the Ga–O ones and, conversely, a shortening of the As–O ones in the neutron refinement. At 295 K, the mean value of Ga–O becomes equal to 1.824 Å, instead of *1.771* Å in the previous X-ray study, in very good agreement with Shannon and Prewitt's compiled values (5) (Ga–O = 1.82 Å). Similarly, the [As–O] bond length refines to 1.674 Å, instead of *1.721* Å, compared to the theoretical value of 1.68 Å. Under these conditions, since all the tetrahedral angles are in good agreement in both structural determinations, the same lengthening and shortening are observed for the O–O edges.

As the atomic coordinates of the "heavy" atoms (Ga and As) from the neutron refinements are in accordance with those previously obtained by X-ray diffraction (1) (Table 3),

TABLE 4
Fractional Thermal Displacement Parameters (Å²) for $GaAsO_4$ from the Neutron (**) and X-ray Refinements

T (K)	U_{11}Ga	U_{22}Ga	U_{33}Ga	U_{23}Ga	U_{11}As	U_{22}As	U_{33}As	U_{23}As
15**	0.00202(11)	0.00198(14)	0.00201(14)	− 0.00009(10)	0.00210(12)	0.00177(16)	0.00183(15)	− 0.00009(11)
295**	0.00865(7)	0.00740(9)	0.00711(9)	− 0.00068(6)	0.00807(7)	0.00641(9)	0.00656(9)	− 0.00048(6)
289	0.0083(4)	0.0090(6)	0.0081(4)	− 0.0010(3)	0.0096(4)	0.0062(5)	0.0068(4)	0.0003(3)
373	0.010(6)	0.011(8)	0.0099(6)	− 0.0019(5)	0.0123(6)	0.0083(7)	0.0079(6)	0.0007(4)
473	0.014(6)	0.013(8)	0.013(6)	− 0.0017(5)	0.0150(6)	0.0112(8)	0.0109(5)	0.0002(4)
573	0.018(7)	0.016(9)	0.015(5)	− 0.0016(5)	0.0172(6)	0.0138(8)	0.0134(5)	− 0.0002(4)
673	0.021(7)	0.019(9)	0.018(5)	− 0.0012(5)	0.0208(6)	0.0163(8)	0.0158(5)	− 0.0006(4)
773	0.025(8)	0.02(1)	0.021(6)	− 0.0018(5)	0.0233(7)	0.0188(9)	0.0183(5)	− 0.0005(5)
873	0.029(8)	0.02(1)	0.023(6)	− 0.0021(6)	0.0262(8)	0.0217(9)	0.0211(6)	− 0.0006(5)
973	0.032(9)	0.03(1)	0.026(6)	− 0.0023(6)	0.0287(8)	0.023(1)	0.0233(6)	− 0.0003(5)
1073	0.03(1)	0.03(1)	0.029(7)	− 0.0030(7)	0.0334(9)	0.025(1)	0.0264(6)	− 0.0004(6)

T (K)	$U_{11}O_1$	$U_{22}O_1$	$U_{33}O_1$	$U_{12}O_1$	$U_{13}O_1$	$U_{23}O_1$	$U_{11}O_2$	$U_{22}O_2$	$U_{33}O_2$	$U_{12}O_2$	$U_{13}O_2$	$U_{23}O_2$
15**	0.00552(14)	0.00395(13)	0.00432(12)	0.00311(11)	− 0.00111(9)	− 0.00138(10)	0.00574(15)	0.00372(14)	0.00446(13)	0.00327(11)	− 0.00089(10)	− 0.00109(11)
295**	0.01784(11)	0.01311(9)	0.01145(9)	0.01064(8)	− 0.00459(7)	− 0.00442(6)	0.01810(11)	0.01255(9)	0.01202(9)	0.01073(8)	− 0.00471(7)	− 0.00424(7)
289	0.023(3)	0.014(2)	0.011(2)	0.018(2)	0.006(1)	0.006(1)	0.015(3)	0.016(2)	0.014(1)	0.009(2)	− 0.004(1)	− 0.006(1)
373	0.019(3)	0.018(3)	0.016(3)	0.016(3)	0.004(2)	0.004(2)	0.030(4)	0.025(3)	0.015(2)	0.019(3)	− 0.008(2)	− 0.008(2)
473	0.030(4)	0.026(4)	0.019(2)	0.023(3)	0.007(2)	0.006(2)	0.030(4)	0.020(3)	0.021(2)	0.019(3)	− 0.007(2)	− 0.009(2)
573	0.040(4)	0.027(4)	0.021(2)	0.027(3)	0.008(2)	0.010(2)	0.038(4)	0.031(3)	0.022(2)	0.024(4)	− 0.009(2)	− 0.011(2)
673	0.046(5)	0.035(4)	0.025(2)	0.033(4)	0.010(2)	0.011(2)	0.042(5)	0.034(3)	0.026(2)	0.027(4)	− 0.010(2)	− 0.011(2)
773	0.052(5)	0.039(4)	0.027(3)	0.034(4)	0.012(2)	0.013(2)	0.051(5)	0.039(4)	0.030(2)	0.032(4)	− 0.011(2)	− 0.012(2)
873	0.060(6)	0.044(4)	0.035(3)	0.041(5)	0.012(3)	0.014(2)	0.059(6)	0.042(4)	0.034(2)	0.036(5)	− 0.012(3)	− 0.012(2)
973	0.069(6)	0.048(4)	0.040(3)	0.047(5)	0.012(3)	0.017(2)	0.059(6)	0.046(4)	0.040(3)	0.035(5)	− 0.014(3)	− 0.014(3)
1073	0.081(8)	0.052(5)	0.045(6)	0.053(6)	0.013(3)	0.017(3)	0.068(7)	0.051(5)	0.045(3)	0.039(5)	− 0.015(3)	− 0.015(3)

Note. The form of the displacement factor was $\exp(-2\pi^2 \sum_i \sum_j U_{ij} \mathbf{h}_i \mathbf{h}_j a^*_i a^*_j)$.

TABLE 5
Bond Distances (Å) and Angles (°) of $GaAsO_4$ from Neutron (*) and X-Ray Diffraction Measurements at Various Temperatures

T (K)	Ga–O_1 (Å)	Ga–O_2 (Å)	O_1–Ga–O_1 (°)	O_1–Ga–O_2 (°)	O_1–Ga–O_2 (°)	O_2–Ga–O_2 (°)
15*	1.8239(4)	1.8346(4)	109.52(3)	112.84(2)	104.59(2)	112.63(3)
295*	1.8187(3)	1.8293(3)	109.48(2)	112.65(1)	104.74(1)	112.74(2)
293	*1.766*	*1.776(5)*	*109.1(4)*	*113.0(3)*	*104.8(2)*	*112.2(4)*
298	1.826(5)	1.835(5)	109.5(2)	112.5(2)	104.8(2)	113.0(2)
373	1.819(7)	1.832(7)	109.2(3)	112.4(3)	104.9(3)	113.3(3)
473	1.826(7)	1.833(7)	109.5(3)	112.1(3)	105.2(3)	112.9(3)
573	1.818(7)	1.835(7)	109.6(3)	112.2(3)	105.0(3)	113.0(3)
673	1.825(7)	1.831(7)	109.4(3)	111.8(3)	105.3(3)	113.3(3)
773	1.822(8)	1.829(8)	109.4(4)	111.9(4)	105.2(4)	113.3(4)
873	1.820(8)	1.828(8)	109.3(4)	111.9(4)	105.4(4)	112.9(4)
973	1.817(9)	1.830(9)	108.8(4)	111.8(4)	105.5(5)	113.4(4)
1073	1.82(1)	1.83(1)	109.3(5)	111.4(5)	105.8(5)	113.1(5)
T (K)	As–O_1 (Å)	As–O_2 (Å)	O_1–As–O_1 (°)	O_1–As–O_2 (°)	O_1–As–O_2 (°)	O_2–As–O_2 (°)
15*	1.6785(5)	1.6810(4)	109.83(3)	112.90(2)	106.99(2)	107.29(3)
295*	1.6720(3)	1.6754(3)	109.88(2)	112.79(1)	107.05(1)	107.36(2)
293	*1.717(5)*	*1.725(6)*	*110.5(4)*	*112.3(3)*	*106.8(3)*	*108.2(4)*
289	1.670(3)	1.665(4)	110.0(2)	112.7(2)	107.1(2)	107.2(3)
373	1.679(5)	1.667(6)	109.8(3)	112.5(3)	107.3(3)	107.6(4)
473	1.669(5)	1.661(6)	110.0(3)	112.7(3)	107.0(3)	107.5(4)
573	1.671(5)	1.665(6)	110.2(3)	112.3(3)	107.4(3)	107.2(4)
673	1.668(5)	1.662(6)	110.2(3)	112.4(4)	107.1(3)	107.7(4)
773	1.668(5)	1.669(7)	110.2(4)	112.3(4)	107.3(3)	107.5(5)
873	1.668(6)	1.668(8)	110.2(4)	112.3(4)	107.4(3)	107.2(5)
973	1.673(6)	1.667(8)	109.8(4)	112.1(4)	107.7(3)	107.4(5)
1073	1.666(6)	1.661(9)	110.4(5)	112.1(5)	107.4(4)	107.5(6)

Note. Previous refinement from X-ray data (1) are in italics.

their interatomic distances are nearly identical ([3.165] and [3.164] Å, respectively). Conversely, in the previous X-ray investigation, the similarity of the atomic scattering factors ($Ga^{3+} = As^{5+} = 28$ electrons) and of their atomic coordinates (only separated by $c/2$) led to a pseudo-extinction for hkl reflections with $l = 2n + 1$. This lack of information affected the accurate localization of the "light" oxygen atoms (O_1 and O_2), themselves also $c/2$ separated, leading to an averaging of the Ga–O and As–O bond lengths ($1.82 + 1.68/2 = 1.75$ Å). However, in neutron diffraction, the scattering lengths for Ga, As, and O are quite distinct; thus all the $l = 2n + 1$ reflections could be measured and all the atomic coordinates very accurately refined (Table 3).

Another similarity between the X-ray and neutron structure refinements is the near equivalence of the average value of the Ga–O–As angle ([129.6°] and [*129.9*°], respectively, at room temperature (Table 6). Since, for all the quartz and quartz-like materials, this bridging angle can be related to their physical properties such as the existence of the α-β transition, the density, the coupling coefficient of the AT-cut and its thermal behavior, further X-ray crystal structure refinements of $GaAsO_4$ have been carried out from room temperature up to 1073 K.

X-ray Diffraction Refinements

Tables 5 and 6 summarize the characteristic angles and bond distances encountered in the $GaAsO_4$ crystal structure

TABLE 6
Intertetrahedron Angles Ga–O–As (°) of $GaAsO_4$ from Neutron (*) and X-Ray Diffraction Measurements at Various Temperatures

T (K)	Ga–O_1–As (°)	Ga–O_2–As (°)
15*	129.53(2)	128.39(2)
295*	130.09(2)	129.10(2)
293	*130.6(4)*	*129.2(4)*
289	130.0(3)	129.1(3)
373	130.4(4)	129.5(4)
473	130.5(4)	130.1(4)
573	131.1(4)	130.0(4)
673	131.0(4)	130.7(4)
773	131.4(4)	130.7(5)
873	131.6(5)	131.0(5)
973	131.8(5)	131.4(5)
1073	132.4(6)	132.2(6)

Note. Previous refinement from X-ray data (1) are in italics.

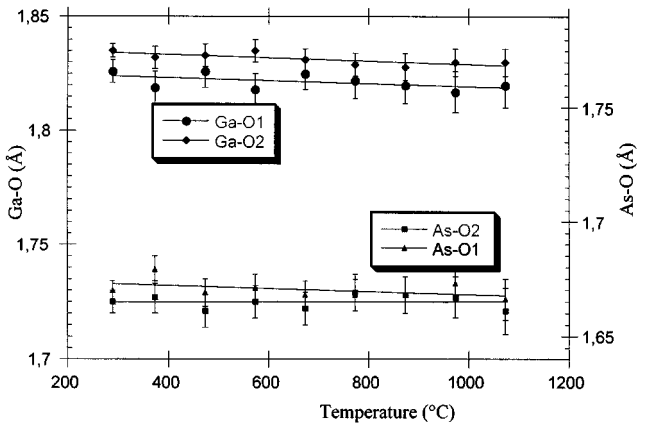

FIG. 2. Evolution of the Ga–O and As–O bond distances with temperature.

deduced from the nine new X-ray data collections between room temperature and 1073 K. Conversely to the previous X-ray determination (1), no drastic bond distance differences were observed between the new X-ray refinements and the neutron refinements ($[Ga–O]_{X\text{-}ray} = 1.830$ Å and $[Ga–O]_N = 1.825$ Å at room temperature. In the old X-ray investigation, only one reflection $l = 2n + 1$ with $I > 3\sigma(I)$ was observed while, in this new room temperature study, 41 weak ($I > 3\sigma(I)$) but significant odd-l reflections where measured. This difference, due to a better crystal and/or more advanced X-ray equipment, can explain the more precise refinement of light oxygen atom coordinates. Moreover, the GaO_4 and AsO_4 tetrahedra are outstandingly stable without any change of their intratetrahedron angle values, nor even a weak shortening of the Ga–O and As–O bond distances (Fig. 2) over the whole temperature range 289–1073 K. Thus, the very weak change in the cell volume (from 246.1 to 253.2 $Å^3$, 2.6%)) is only due to the [Ga–O–As] intertetrahedron angle variation from 129.55° to 132.3° (2.6%) (Fig. 3 and Table 6).

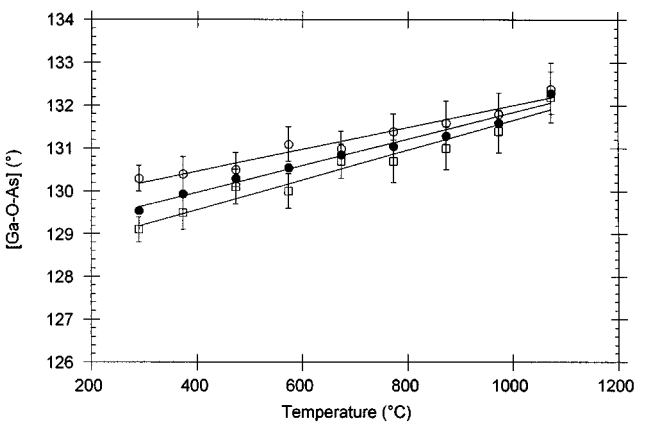

FIG. 3. Evolution of the angles Ga–O(1)–As [○] and Ga–O(2)–As [□] and their mean value with temperature.

In summary, very accurate Ga–O and As–O bond lengths were obtained from neutron data refinement and were confirmed by high-temperature X-ray measurements using more advanced equipment than used previously (1). Thus, the old distances were simply incorrect due to a lack of precision in the previous data collection. It appears that the crystal structure of $GaAsO_4$ exhibits only very slight changes over a wide range of temperatures and it is therefore interesting to compare its stability to the other quartz-like crystal structures: SiO_2, GeO_2, and MXO_4 with M = Al, Ga, Fe and X = P, As.

DISCUSSION

Distortion Measurement of Quartz-Like Structures: Bridging Angle θ, Tilt Angle δ, and Parameter Ratio c/a

As already mentioned (3), the structural deformation of α-quartz and its homeotypes can be expressed by simply the averaged value of the intertetrahedron angles (θ) which is close to 154° for the nondistorted β-quartz (4) or by its corollary, the averaged value of the "tilt angle," δ, which is the rotational shift of the tetrahedra from the ideal β-quartz position where $\delta = 0$ (Fig. 4).

The more distorted is the structure, the more the θ and δ values decrease and increase, respectively. The relation between these two parameters is given by (16):

$$\cos\theta = \frac{3}{4} - \left[\cos\delta + \frac{1}{2\sqrt{3}}\right]^2 \qquad [1]$$

which, to a first approximation, is a linear relation for the quartz and quartz-like materials at room temperature (3). However, the linear approximation is not so good when the available data over all the pressure and the temperature conditions of the crystal structure measurements are considered (1, 4, 17–23) (Fig. 5). While, for intermediate distortions, the experimental values fit very well the theoretical

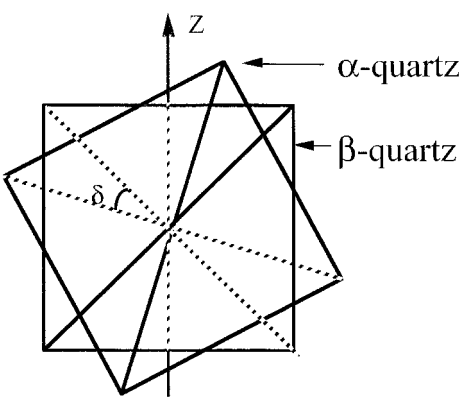

FIG. 4. "Tilt angle," δ, related to the rotation angle between α- and β-quartz structures.

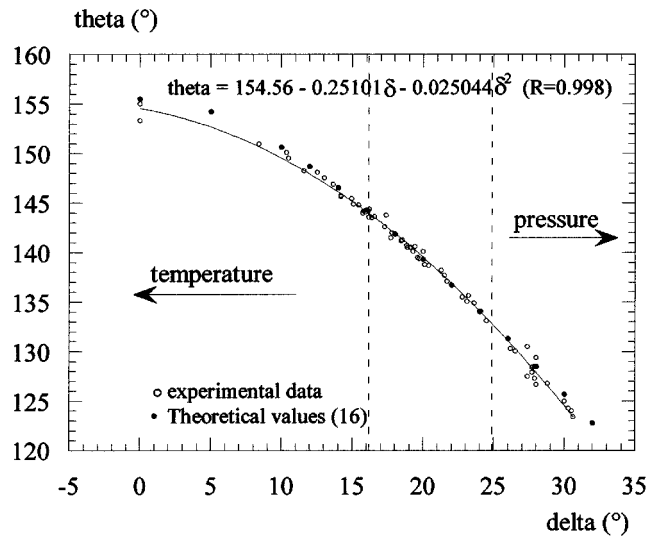

FIG. 5. Tilt angle, δ, for all available data in terms of pressure and temperature with the central linear part observed at room temperature (between the vertical dashed lines).

ones calculated from Eq. [1], slight deviations are observed for weakest distortions obtained at high temperature (close to β-quartz $\approx 154^\circ$ (4)) and strongest distortions obtained under pressure. Therefore, all the data were fitted with a second-order polynomial law to give a very good agreement between these two parameters over the whole range studied thus far.

The accurate knowledge of the parameters θ and δ, and their thermal behavior, is of major interest to anticipate the physical properties for quartz-like crystals which have not yet been synthesized in sizes large enough to be characterized directly (3). For example, when the distortion increases, the necessary energy for the α-β transition (i.e., change of M–O–X angle toward 154°) and, thence, the transition temperature, increase also. In this case, other phase transitions (e.g., α-quartz–cristobalite, as occurs at 1206 K for $GaPO_4$) or chemical decomposition may be observed (24). The limit for which the α-β transition is possible was found to be $\delta = 22^\circ$ and $\theta = 136^\circ$ at room temperature and pressure (2).

The structure deformations can also be estimated from the difference of the c/a ratio from 1.0981 which is the ideal value for nondistorted quartz structure (25). If we consider all the available crystal structure data, over temperature and pressure (1, 4, 17–23, 26–34), and we plot c/a versus θ, all the data cannot be fitted by only one curve (Fig. 6).

While the corresponding data for SiO_2, GeO_2, and $AlAsO_4$ follow the same evolution, the evolution for other MXO_4 compounds is slightly shifted toward higher c/a ratio values. The only possible explanation for this shift is the difference in the tetrahedron volumes, MO_4 and XO_4, which, to a first approximation, are related to their bond lengths, M–O and X–O, respectively. If we compare the $(M\text{–O})/(X\text{–O})$ ratio of all the known compounds at room temperature and ambient pressure, this ratio increases from SiO_2 to $FePO_4$:

SiO_2	GeO_2	$AlAsO_4$	$GaAsO_4$	$AlPO_4$	$GaPO_4$	$FePO_4$
1.0	1.0	1.04	1.10	1.14	1.19	1.21

We observe two different ranges, the first close to 1.0 for the first three compounds and the second between 1.10 and 1.21 for the four other compounds (Fig. 6). In other words, for the same θ value, the crystal structure becomes more and more distorted as the difference between the M–O and X–O bond distance increases.

Comparative Piezoelectric Behavior of Quartz and Quartz-Like Materials

Of all these compounds, only three of them are known definitely to be piezoelectric: SiO_2, $AlPO_4$, and $GaPO_4$. For the other materials, sufficiently large crystals are not yet available for piezoelectric characterization. Nevertheless, from the first three known phases, some piezoelectric behavior can be foreseen for the other ones and also their stability versus temperature and pressure predicted.

(*a) Relation between structural deformations and piezoelectric behavior.* First, if we consider the three well-known compounds, SiO_2, $AlPO_4$, and $GaPO_4$, each of them exhibits a temperature-compensated cut, AT, i.e., a cut orientation where the resonance frequency is not modified by temperature. Wafers of these materials are characterized by

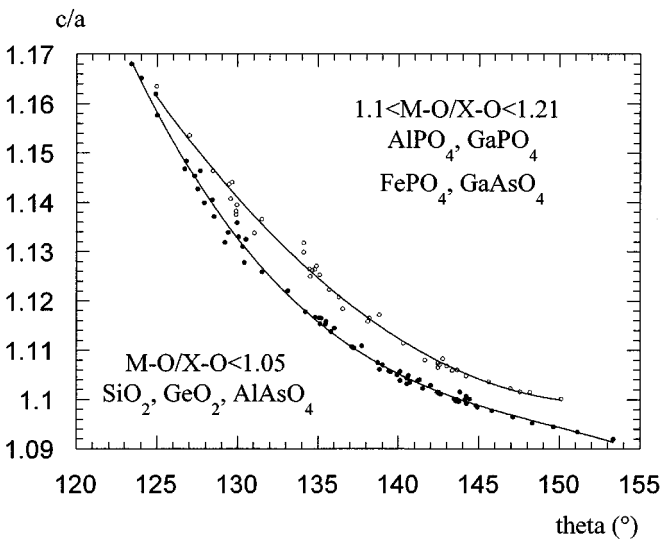

FIG. 6. Relation between c/a ratio and the M–O–X angle. For the MXO_4 phases, the c/a ratio was divided by 2.

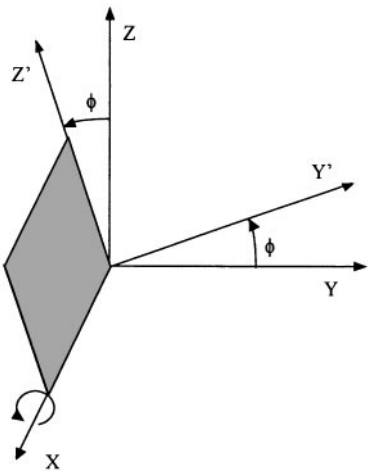

FIG. 7. *Y*-rotated cut from IEEE-78 (35).

their cut angle ϕ (*Y*-rotated cut; Fig. 7) and their piezoelectric coupling coefficient k (or piezoelectric yield). The coupling coefficient and the *Y*-rotated angle value for the three known compounds in terms of the *M*–O–*X* angle are plotted in Fig. 8. Both parameters are linearly related to the structural deformation expressed by θ. Second, the coupling coefficient value must be equal to zero for $\theta \approx 154°$, which is the mean value found for the Si–O–Si angle in β-quartz (4, 36) which, although noncentrosymmetric, does not exhibit piezoelectric behavior (37).

Thus, from the linear relation of ϕ and k, piezoelectric properties of the AT-cuts can be extrapolated for crystals for which the crystal growth does not yet permit piezoelectric characterization. For example, the known structural distortions of $AlAsO_4$, GeO_2, and $GaAsO_4$ allow us to deduce their piezoelectric behavior:

— $AlAsO_4$ should be similar to $GaPO_4$.

— The structures with the most distorted packing, GeO_2 and $GaAsO_4$, should exhibit the most promising coupling coefficient, $k \approx 21\%$, and a *Y*-rotated angle close to $-5°$.

As piezoelectric devices are often used under extreme conditions and their properties are related to their structure stability, we also need to consider their behavior with temperature and pressure.

(*b) Thermal behavior of $GaAsO_4$ compared to other quartz-like materials.* An ideal piezoelectric material must exhibit, as well as a high coupling coefficient, a high thermal stability of its piezoelectric properties which is related to its structural stability. Generally, the thermal stability of a phase depends on its domain of existence and, in this temperature domain, on the variation of its structural packing. For quartz and quartz-like materials, this last change can be estimated by the evolution of the tilt angle, δ, (or the *M*–O–*X* angle, θ) (Fig. 9).

For the first criterion, the temperature range of the α-quartz structure stability increases with the tilt angle, i.e., with the distortion. Indeed, if the α-quartz structure is limited at 846, 859, and 980 K for quartz (38), $AlPO_4$ (24), and $FePO_4$ (24), respectively, it persits until 1206 K for $GaPO_4$ (24) and exceeds 1300 K for the most distorted materials, GeO_2 (39) and $GaAsO_4$ (24). In the same way, the dependence of the tilt angle for three of these phases, $GaPO_4$, $AlAsO_4$, and $GaAsO_4$, (data for GeO_2 are not available yet, but can be predicted; see below) exhibits a linear behavior, with an absolute value of the slope which decreases from $AlAsO_4$ to $GaAsO_4$ ($|3.43|$ to $|1.96| \times 10^{-3}$, respectively). Thus the packing stability increases with the structural

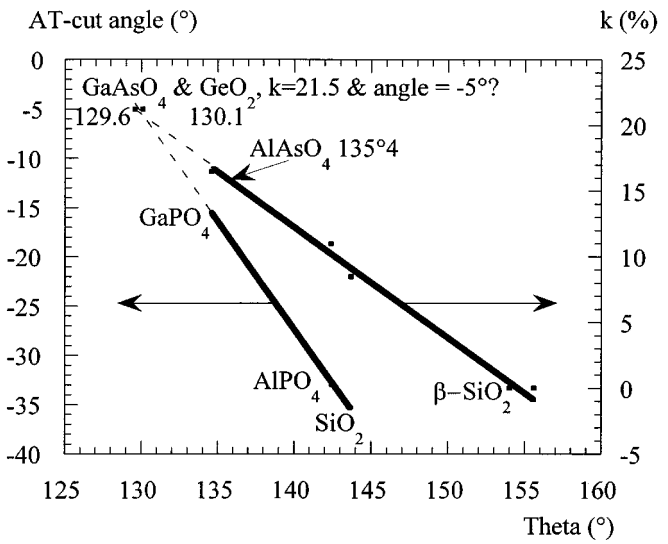

FIG. 8. Coupling coefficient (k) and angle of the AT-cuts in terms of the bridging angle *M*–O–*X*.

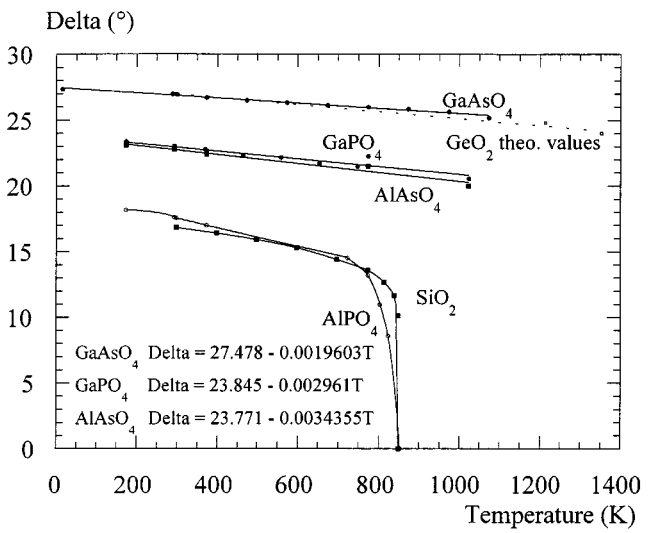

FIG. 9. Evolution of the tilt angle, δ, with temperature.

deformation. In conclusion, compared to other quartz-like materials, $GaAsO_4$ seems to be the most promising compound for piezoelectric devices needing a wide temperature range with high thermal stability.

(*c) Predicted thermal behavior of GeO_2.* From previous relations between the different structural packing distortions, it is possible to foresee the thermal stability of a material from only its cell parameters. For example, a recent powder X-ray investigation of GeO_2 was carried out from room temperature to 1353 K (39). The c/a evolution can be related successively to the Ge–O–Ge bridging angle (Fig. 6), to the tilt angle (relation [1]) and, thus, the thermal sensitivity (Table 7 and Fig. 9) can be predicted. The slope of the linear evolution of the tilt angle for GeO_2 in terms of temperature ($|2.5| \times 10^{-3}$) exhibits a value between those of $GaPO_4$ and $GaAsO_4$ and, thus, the thermal sensitivity of its piezoelectric properties should also be between those of $GaPO_4$ and $GaAsO_4$. This behavior needs to be confirmed by high temperature X-ray measurements on a single crystal.

(*d) Pressure stability of quartz like materials.* Very few X-ray measurements under pressure have been carried out on quartz-like materials, except for quartz itself. Nevertheless, some interesting results can be observed. Figure 10 summarizes the pressure behavior of such materials (26–34).

All the data can be very well fitted with a second-order polynomial law except for one SiO_2 investigation (34). If we compute the pressure values where the derivatives of these curves are equal to zero (corresponding to no change in the tilt angle δ), it can be considered that this pressure value is the limit of the α-quartz type domain before transformation to another crystal structure or amorphization. From the equations given in Fig. 10, these values increase from GeO_2 (9 GPa) to SiO_2 (15–25 GPa (30, 34)). These results are in good agreement with the experimental data obtained from different techniques (X-ray diffraction, X-ray absorption, IR, theoretical calculations, etc.), such as 8–9 GPa for GeO_2 (30), $AlAsO_4$ (28, 32), and $GaAsO_4$ (40), 14 GPa for $GaPO_4$ (29), 15 GPa for $AlPO_4$ (27), and 15–25 GPa for SiO_2 (30,34). In contrast to the thermal behavior, the pressure stability increases with the mean value of the ionic bond character, from GeO_2 (0.511) to SiO_2 (0.570) (41). As the mean value of $GaAsO_4$, calculated from (41), is 0.511, this material must exhibit a pressure sensitivity similar to that of GeO_2 ($\approx$ 9 GPa) in agreement with the experiments (9 Gpa in (40)).

TABLE 7
Thermal Behavior of GeO_2

Temperature (K)	c/a	Ge–O–Ge (°)	Tilt angle (°)
293	1.134	129.8	27.0
773	1.130	130.8	26.3
1213	1.122	133.0	24.8
1353	1.118	134.0	24.0

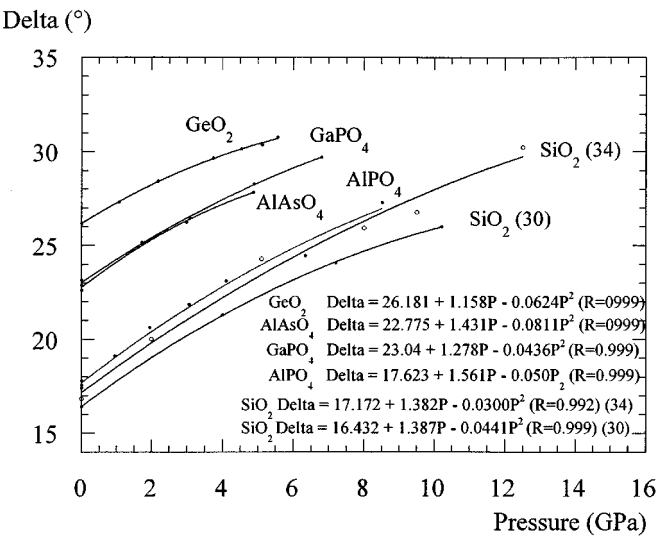

FIG. 10. Evolution of the tilt angle, δ, with pressure.

CONCLUSION

The neutron crystal structure investigation allowed a very accurate determination of the Ga–O and As–O bond lengths in $GaAsO_4$ in contrast to a previous X-ray refinement which had a tendency to average them. A new set of X-ray data, collected with state-of-the-art equipment, led to values which are in accordance with those obtained by neutron diffraction. Consequently, further X-ray measurements of a $GaAsO_4$ crystal have been carried out in the temperature range 289 to 1073 K. This new structural investigation has emphasized the high thermal stability of the α-quartz packing in $GaAsO_4$, the best amongst quartz-like materials.

Furthermore, the experimental relation between structural deformations and piezoelectric properties of these materials allows us to predict that $GaAsO_4$ should have the best piezoelectric characteristics for its AT-cut. Its high coupling coefficient and its weak thermal sensitivity make this material very promising. Thus, we have undertaken its crystal growth in order to confirm these predictions. In contrast, its higher covalent character should imply a greater pressure sensitivity, with a crystal structure transition around 9 GPa. Thus, it is the best piezoelectric candidate for high-temperature applications but not for high-pressure devices.

REFERENCES

1. A. Goiffon, J. C. Jumas, M. Maurin, and E. Philippot, *J. Solid State Chem.* **61,** 384 (1986).

2. E. Philippot, A. Goiffon, A. Ibanez, and M. Pintard, *J. Solid State Chem.* **110,** 356 (1994).
3. E. Philippot, D. Palmier, A. Goiffon, and M. Pintard, *J. Solid State Chem.* **123,** 1 (1996).
4. K. Kihara, *Eur. J. Mineral.* **2,** 63 (1990).
5. R. D. Shannon and C. T. Prewitt, *Acta Cryst.*, *B* **25,** 925 (1969).
6. D. Palmier, A. Goiffon, B. Capelle, J. Détaint, and E. Philippot, *J. Cryst. Growth* **166,** 347 (1996).
7. M.S. Lehmann, W. Kuhs, C. Wilkinson, J. Allibon, and G. J. McIntyre, *J. Appl. Cryst.* **22,** 562 (1974).
8. C. Wilkinson, H.W. Khamis, R. F. D. Stansfield, and G. J. McIntyre, *J. Appl. Cryst.* **21,** 471 (1988).
9. P. Coppens, L. Leiserowitch, and D. Rabinowich, *Acta Cryst.* **18,** 1035 (1965).
10. J. O. Lundgren, Crystallographic Computer Programs, Report UUIC-B13-4-05, Institute of Chemistry, University of Uppsala, Sweden, 1982.
11. V. F. Sears, *Neutron News* **3,** 26 (1992).
12. P. Becker and P. Coppens, *Acta Cryst.*, *A* **30,** 129 (1975).
13. P. Becker and P. Coppens, *Acta Cryst.*, *A* **31,** 417 (1975).
14. Z. Otwinowski and W. Minor, *in* "Methods in Enzymology" (Carter, Jr. and R. M. Sweet, Eds.), Vol. 276, Academic Press, San Diego, 1996.
15. P. Wolfers, *J. Appl. Cryst.* **23,** 554 (1990).
16. H. Grimm and B. Dorner, *J. Phys. Chem. Solids* **36,** 407 (1975).
17. Y. Le Page, L. D. Calvert, and E. J. Gabe, *J. Phys. Chem. Solids* **41,** 721 (1980).
18. O. Baumgartner, A. Preisinger, P. W. Krempl, and H. Mang, *Z. Kristallogr.* **168,** 83 (1984).
19. O. Baumgartner, M. Behmer, and A. Preisinger, *Z. Kristallogr.* **187,** 125 (1989).
20. H. Nakae, K. Kihara, M. Okuno, and S. Hirano, *Z. Kristallogr.* **210,** 746 (1995).
21. H. N. Ng and C. Calvo, *Can. J. Phys.* **54,** 638 (1976).
22. Y. Muraoka and K. Kihara, *Phys. Chem. Minerals* **24,** 243 (1997).
23. A. Goiffon, J. C. Jumas, and E. Philippot, *Rev. Chim. Minér.* **23,** 99 (1986).
24. K. Kosten and H. Arnold, *Z. Kristallogr.* **152,** 199 (1980).
25. G.S. Smith, *Acta Cryst.*, *B* **25,** 542 (1963).
26. K. Ogata, Y. Takéuchi, and Y. Kudoh, *Z. Kristallogr.* **179,** 403 (1987).
27. H. Sowa, J. Macavei, and H. Schulz, *Z. Kristallogr.* **192,** 119 (1990).
28. H. Sowa, *Z. Kristallogr.* **194,** 291 (1991).
29. H. Sowa, *Z. Kristallogr.* **209,** 954 (1994).
30. J. Glinemann, H. E. King, H. Schulz, Th Hahn, S. J. La Placa, and F. Dacol, *Z. Kristallogr.* **198,** 172 (1992).
31. J. D. Jorgensen, *J. Appl. Phys.* **49**(11), 5473 (1978).
32. H. Sowa and H. Ahsbahs, *Z. Kristallogr.* **211,** 96 (1996).
33. L. Levien, C. T. Prewitt, and D. J. Weidner, *Amer. Mineral.* **65**, 920 (1980).
34. R. M. Hazen, L. W. Finger, R. J. Hemley, and H. K. Mao, *Solid State Com.* **72**(5), 507 (1989).
35. IEEE Standard on piezoelectricity, Inc., 345 East 47th Street, New York, NY 10017, 1978.
36. A. F. Wright and M. S. Lehmann, *J. Solid State Chem.* **36,** 371 (1981).
37. G. Dolino, J. P. Bachheimer, F. Gervais, and A. F. Wright, *Bull. Minéral.* **106,** 267 (1983).
38. T. Rey, *Z. Kristallogr.* **123,** 263 (1966).
39. P. Yot, O. Cambon, A. Goiffon, and E. Philippot, to be published.
40. J. Badro, Ph. Gillet, P. F. McMillan, A. Polian, and J. P. Itié, *Europhys. Lett.* **40** (5), 533 (1997).
41. B. F. Levine, *J. Chem. Phys.* **59**(3), 1463 (1973).